

# OpenDAS: Domain Adaptation for Open-Vocabulary Segmentation

Gonca Yilmaz<sup>1,2</sup> \* Songyou Peng<sup>1</sup> Francis Engelmann<sup>1,3</sup> Marc Pollefeys<sup>1,4</sup> Hermann Blum<sup>1,5</sup>

<sup>1</sup> ETH Zurich <sup>2</sup> University of Zurich <sup>3</sup> Google <sup>4</sup> Microsoft <sup>5</sup> Lamarr Institute / Uni Bonn

## Abstract

The advent of Vision Language Models (VLMs) transformed image understanding from closed-set classifications to dynamic image-language interactions, enabling Open-Vocabulary Segmentation (OVS). Despite this flexibility, VLMs often fall behind closed-set classifiers in accuracy due to their reliance on ambiguous image captions and lack of domain-specific knowledge. We, therefore, introduce a new task *domain adaptation for open-vocabulary segmentation*, enhancing VLMs with domain-specific priors while preserving their open-vocabulary nature. Existing adaptation methods, when applied to segmentation tasks, improve performance on training queries but can reduce VLM performance on zero-shot text inputs. To address this shortcoming, we propose an approach that combines parameter-efficient prompt tuning with a triplet-loss-based training strategy. This strategy is designed to enhance open-vocabulary generalization while adapting to the visual domain. Our results outperform other parameter-efficient adaptation strategies in open-vocabulary segment classification tasks across indoor and outdoor datasets. Notably, our approach is the only one that consistently surpasses the original VLM on zero-shot queries. Our adapted VLMs can be seamlessly integrated into existing OVS pipelines, improving OV-Seg by +6.0% mIoU on ADE20K, and OpenMask3D by +4.1% AP on ScanNet++ Offices without any changes to the methods.

## 1 Introduction

Recent developments in Vision Language Models (VLMs), such as CLIP [39] and ALIGN [18], catalyzed a paradigm shift in image understanding. These models have enabled significant advances in detecting, localizing, and segmenting images given open-vocabulary queries. Methods for Open-Vocabulary Segmentation (OVS) demonstrated the ability to leverage the generalization capabilities of VLMs, allowing them to be applied ‘zero-shot’ to any image. This had transformative impact on practical applications, ranging from autonomous home robots [28, 34, 50, 67], capable of understanding textual commands for object interaction [6], to systems like Text2Loc [52], SceneGraphLoc [36] and Language Frontier Guide [42], facilitating localization and navigation in unfamiliar environments.

Unfortunately, VLMs’ efficacy in tasks like scene segmentation and object identification in response to text prompts remains suboptimal compared to domain-specific models that are supervised with a given, fixed set of categories. A primary obstacle to enhancing the performance of VLMs is their reliance on extensive datasets for learning a comprehensive representation space. Although this contributes to their strong generalization capabilities, it also limits their effectiveness in specialized domains where tasks like semantic segmentation become more fine-grained. For example, CLIP-based approaches have problems to distinguish “door” and “door frame” in an image.

To overcome this challenge, we introduce a new paradigm, namely “domain adaptation for open-vocabulary segmentation”. The goal is to improve language-queried object segmentation by adapting VLMs to a visual target domain and a style of input prompt, while retaining generalization to novel

\*corresponding author: gyilmaz@student.ethz.ch

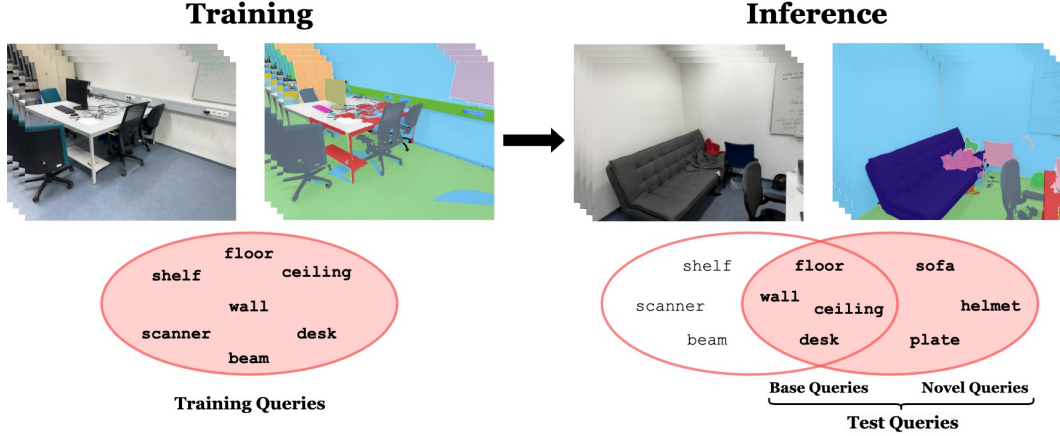


**Figure 1: Domain Adaptation for Open-Vocabulary Segmentation.** We introduce a new task, *domain adaptation for open-vocabulary segmentation*. We learn from ground truth masks and training (base) queries. In inference, we test our model with visually closer domains with unseen queries, showing its generalization capabilities while still adapting to the domain.

language queries. This aligns closely with practical applications where open-vocabulary segmentation has shown promising impacts. For instance, it is both reasonable and expected for a home robot to adapt to its environment while still being able to understand and act upon arbitrary language prompts.

In this work, we investigate approaches for domain adaptation for open-vocabulary segmentation that take SOTA architectures in open-vocabulary segmentation but replaces their CLIP-based foundation with a plug-and-play adapted VLM. These approaches therefore adapt a CLIP-based model to better match text and image crops, *independently* of mask predictions. To adapt CLIP into a specific domain, we leverage prompt tuning, a new, parameter-efficient technique to adapt VLMs that is shown to be effective for task adaptation [19, 22–24, 27, 64, 65] and domain adaptation [11, 12, 20]. We adopt such methods for the first time to inject domain priors for 2D and 3D segmentation tasks.

Our experiments reveal that VLMs adapted with existing prompt-tuning methods for the task of segment classification can unfortunately degrade their ability to generalize zero-shot to novel text queries. However, the goal of domain adaptation for OVS is to improve the response to novel queries through injection of domain knowledge. We therefore propose OpenDAS, a new method that adopts a multimodal prompt tuning architecture, but combines it with a triplet loss based training strategy for text queries. Compared to only using greedy cross-entropy loss, our proposed approach appears to boost the VLM’s generalization capabilities towards unseen queries during the adaptation.

With extensive experiments in 3 challenging datasets, from indoor to outdoor scenes, our approach proves to yield better performance over other parameter-efficient adaptation strategies, and is also the most effective to improve the VLMs performance also on the zero-shot generalisation to novel queries. Moreover, we demonstrate that our method can readily be integrated into existing OVS methods, boosting scene understanding capabilities in 2D and 3D settings.

In summary, our main contributions are as follows:

- We introduce a new task, namely domain adaptation for open vocabulary segmentation.
- We distill prior approaches on prompt-tuning into a simple yet effective model architecture for segment classification and pair it with a new triplet-loss-based training strategy to further boost open-vocabulary understanding of the adapted model.
- Our method significantly outperforms previous unimodal and multimodal methods and also surpasses the original CLIP model’s generalization to novel text queries in the target domain.

## 2 Related Work

**2D Open-Vocabulary Segmentation.** 2D Open-Vocabulary Segmentation (OVS) involves localizing objects in images from language cues. The common approach is to generate class-agnostic masks and visual embeddings, then compare them to VLM text embeddings [49]. LSeg [30] uses CLIP text embeddings and aligns pixel-level features to the semantic class, while OpenSeg [13] aligns segment-level features with text embeddings via region-word grounding. Other approaches also

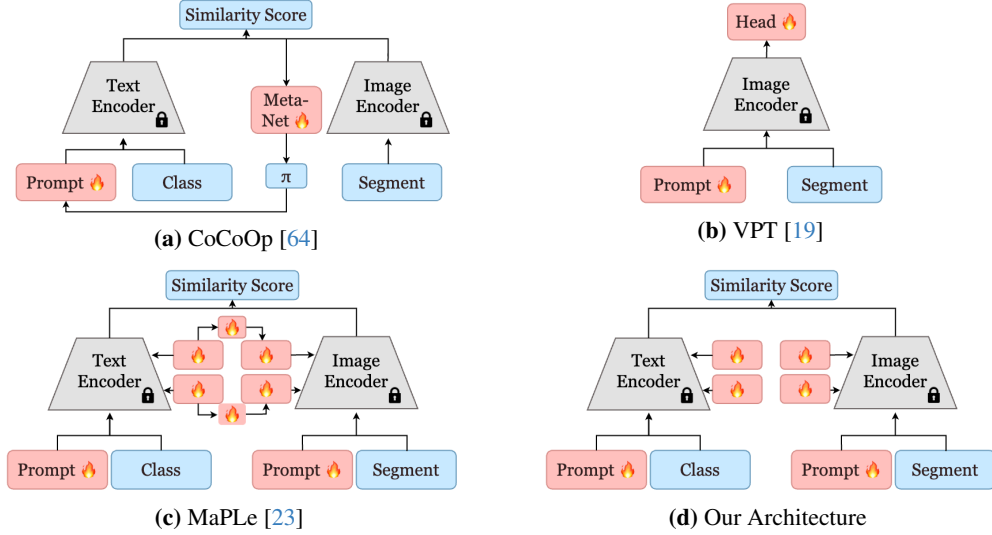


**Figure 2: Model Architecture Comparison.** We compare our architecture against the existing prompt tuning methods. All text and image encoders are frozen and learnable parameters are marked with 🔥. CoCoOp (Fig. 2a) adds dynamic text prompts based on image features, while VPT (Fig. 2b) only adds learnable prompts to the visual encoder. MaPLe (Fig. 2c) adds prompts to visual and textual encoders combined with a coupling layer.

rely on CLIP to generate textual embeddings and encode images or segments in the same latent space [5, 7, 8, 32, 54, 62]. These methods require reliable zero-shot segment classification, but their performance is limited by CLIP’s capabilities, even with ground truth masks.

**3D Open-Vocabulary Segmentation.** Recent advances in 3D segmentation [26, 41, 46, 47, 59], and inspired by the progress in 2D, are reshaping how we understand complex 3D scenes [3, 9, 21, 25, 38]. As many of these methods rely on CLIP [39], its adaptation to a specific domain could enhance the 3D OVS performance within the target domain. Thus, we demonstrate our adaptation’s potential by applying it to the open-vocabulary 3D instance segmentation method OpenMask3D [45]. This approach utilizes class-agnostic mask proposals [17] and pre-trained CLIP [39] for mask and text embeddings, following the most common design described in [49].

**Prompt Tuning.** Prompt tuning is a method where learnable parameters are added to input and interim encoder layers to enhance model performance in specific tasks or domains. Initially proposed for LLMs [14, 29, 31, 35], it allows for model adaptation with minimal computational costs, overcoming the limitations of full model fine-tuning. Recently, it has been extended to VLMs like CLIP [39], showing promising results [16, 65, 64, 19, 23, 22, 24, 27]. Significant contributions (see Fig. 2) include CoCoOp [64] and VPT [19] as unimodal prompt tuning examples. CoCoOp (see Fig. 2a) adds dynamic textual prompts based on image features, while VPT (see Fig. 2b) adds learnable visual prompts and a linear probe layer. Recent works [24, 27] employ multimodal learning by jointly training textual and visual prompts. MaPLe [23] (see Fig. 2c) couples interim textual and visual prompts. Instead, we use a simpler architecture with separate prompts, enabling sequential learning and full control over adaptation of each modality.

**Domain Adaptation and Downstream Task Adaptation.** Domain adaptation aims to align the disparity between the original training data distribution and the target domain distribution [10]. Recently, prompt tuning methods were adopted for domain adaptation to inject domain priors to the model without exhaustive full model fine-tuning [11, 12, 20]. Moreover, prompt tuning has also been widely used for downstream task adaptation of foundational models in a parameter-efficient manner [19, 43, 64, 65]. Hence, we adopt prompt tuning methods to inject domain priors into VLMs and adapt them to the open-vocabulary segmentation task.

### 3 Domain Adaptation for Open-Vocabulary Segmentation

In this work, we propose the task of ‘domain adaptation for open-vocabulary segmentation’. Like any domain adaptation task, the goal is to enrich an existing model with domain-specific knowledge.

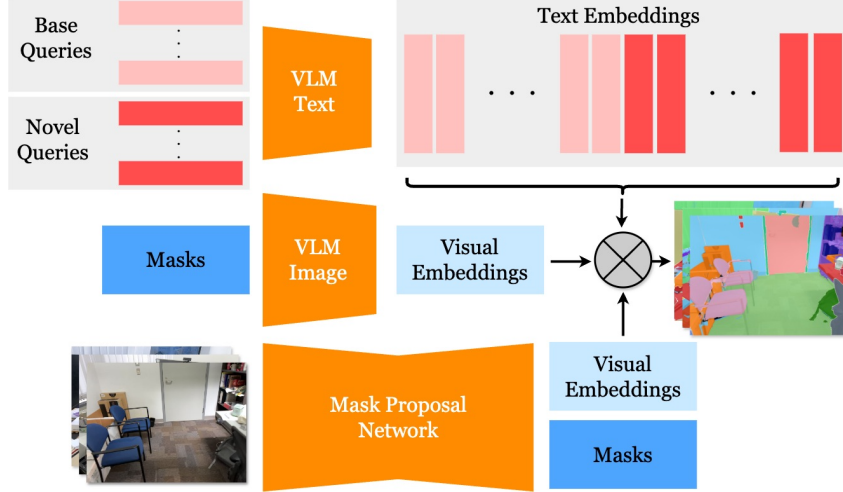


**Figure 3: The Common Pipeline for Open-Vocabulary 2D Segmentation.** As described in the survey [49], the pipeline takes a set of images and generates masks with visual embeddings. The generated masks are fed into a VLM Image Encoder to generate visual embeddings, which are then combined with the remaining pipeline. In parallel, the VLM Text Encoder takes a set of base and novel queries and produces text embeddings. Subsequently, these visual and text embeddings are compared against each other to predict classes for each mask.

In our case, we want to adapt VLMs that are trained on internet-scale data to i) a visual domain e.g. homes and offices or urban driving; ii) the task of segmentation, instead of other tasks that VLMs are used for, such as image captioning or visual Q&A.

At the same time, we aim to retain the model’s open-vocabulary ability, ensuring it can accurately process unseen language queries. This is illustrated in Fig. 1, where the model is exposed to a set of images and queries during training. At inference, it can be queried with any language prompt, requiring open-vocabulary understanding with zero-shot capabilities, as expected from the original VLM. Consequently, adaptation performance needs to be measured over *base* and *novel* queries. Base queries in the test set also appear in the training queries and are typically prevalent in the domain (e.g., ‘car’ in urban driving). Novel queries are zero-shot queries that the model has not seen during adaptation but should understand better because of its adaptation to the visual domain.

## 4 Method

Following the task definition in the previous section, we present a method to adapt CLIP and similar VLMs into a target domain for open-vocabulary segmentation. We first explain the preliminaries required for our method (Sec. 4.1). Next, we propose a simple yet effective way for multimodal prompt tuning (Sec. 4.2), and introduce a novel training strategy based on a triplet loss (Sec. 4.3). Finally, we discuss how to mine data for the triplet loss (Sec. 4.4).

### 4.1 Preliminaries

As shown in Fig. 3, the architecture of common open-vocabulary 2D segmentation pipelines typically comprises: a) a class-agnostic mask proposal component that generates potential masks along with their visual embeddings, and b) a pre-trained VLM text encoder to output text embedding for each class name, and c) optionally, a pre-trained VLM image encoder that also outputs visual embeddings given the mask proposals. Following most open-vocabulary segmentation models, in this paper, we use CLIP [39] with a Vision Transformer (ViT) backbone as the chosen VLM.

The matching between semantic queries and each mask proposal is then given by the cosine similarity between the corresponding visual embedding  $\mathbf{v}$  and text embeddings  $\{\mathbf{t}_1, \dots, \mathbf{t}_N\}$  of all  $N$  queries. The query with the highest score corresponds to the semantic prediction  $\hat{y}$  for this mask, denoted as:

$$\hat{y} = \underset{n}{\operatorname{argmax}} \{\cos(\mathbf{v}, \mathbf{t}_n)\}. \quad (1)$$

Despite demonstrating promising results, open-vocabulary segmentation faces significant challenges, particularly due to the limited domain generalization capabilities of CLIP embeddings. These limitations hinder the segmentation precision across diverse domains (see Fig. 4). Drawing inspiration from the success of multimodal prompt tuning in enhancing classification accuracy across various



domains [65, 64, 23, 27, 19, 32], we propose adopting a novel prompt tuning approach to specifically refine CLIP for improved domain-specific segmentation, as outlined in Sec. 4.2.

## 4.2 Multimodal Prompt Tuning

In prompt tuning, learnable tokens are appended to the user-provided input prompt (usually text or image) of the model. Prompt tuning enables the adaptation of CLIP for target domains by learning the input prompts instead of handcrafting them. The additional tokens appended provide contextual information on target domains while keeping the model parameters fixed. This way, it only introduces a small fraction of new learnable parameters, making the learning process much more efficient.

More specifically, as illustrated in our architecture in Fig. 2d, we first concatenate a set of learnable prompts to image patch embeddings and text embeddings, respectively. After appending the prompt vectors, the enhanced tensors are formed for image visual embeddings, denoted as  $\mathbf{v}^{(0)}$  and text embeddings, denoted as  $\mathbf{t}^{(0)}$ :

$$\mathbf{v}^{(0)} = [\mathbf{v}^{(0)}; \mathbf{e}_v^{(0)}; \mathbf{p}_v^{(0)}] \quad (2)$$

$$\mathbf{t}^{(0)} = [\mathbf{t}^{(0)}; \mathbf{e}_t^{(0)}; \mathbf{p}_t^{(0)}] \quad (3)$$

where  $\mathbf{v}^{(0)}$  and  $\mathbf{t}^{(0)}$  represent [CLS] and [EOS] special token embeddings,  $\mathbf{e}_v^{(0)}$  and  $\mathbf{e}_t^{(0)}$  are the visual and text embeddings.  $\mathbf{p}_v^{(0)} = (\{p_i^v\}_{k=1}^K)^{(0)}$  and  $\mathbf{p}_t^{(0)} = (\{p_i^t\}_{k=1}^K)^{(0)}$  correspond to the learnable prompts added in the input space, where  $K$  is the total number of learnable prompts and  $p_k^v, p_k^t$  are the  $k$ -th learnable prompt. Note that we initialize text prompts,  $\mathbf{p}_t^{(0)}$  with the tokenization of ‘‘A photo of a’’ for the prompts added in the input space, while  $\mathbf{p}_v^{(0)}$  is initialized from a random distribution [23]. Next, we also append such  $K$  learnable prompts into deeper layers as the following:

$$\mathbf{v}^{(j)} = [\mathbf{e}_v^{(j-1)}; \mathbf{p}_v^{(j-1)}] \quad (4)$$

$$\mathbf{t}^{(j)} = [\mathbf{e}_t^{(j-1)}; \mathbf{p}_t^{(j-1)}] \quad (5)$$

where  $\mathbf{v}^{(j)}, \mathbf{t}^{(j)}$  are the input tensors to the  $(j+1)$ -th layer,  $1 < j \leq J$  and  $J$  is the prompt depth. If  $J = 1$ , the model defaults to combining CoOp [65] for the text encoder and VPT-Shallow [19] for the visual encoder.  $J$  is bounded by the total number of layers of the visual/text encoders. If  $J$  is smaller than the total number of layers, for the remaining layers in the encoders after the  $J$ -th layer, we simply feed the preceding layer’s prompt embedding through the remaining layers [23, 27].

## 4.3 Optimization

Here we introduce how we optimize the visual prompts  $\mathbf{p}_v^{(j)}$  and text prompts  $\mathbf{p}_t^{(j)}$  in each layer as discussed in Sec. 4.2. The process commences with the optimization of only visual prompts, and shifts to optimize only text prompts.

**Optimization of Visual Prompts.** In each iteration, we randomly sample a batch of 16 image segments with their annotated class names, passing through the CLIP visual and text encoder to obtain their embedding  $\mathbf{v}_i$  and  $\mathbf{t}_i$  for each segment  $i$ . Following VPT [19], we use a cross-entropy loss  $\mathcal{L}_{ce}(\mathbf{v}_i, \mathbf{t}_i)$  to optimize the visual prompts  $\mathbf{p}_v^{(j)}$  for.

**Optimization of Text Prompts.** Once optimized, we freeze the visual prompts and solely optimize the text prompts  $\mathbf{p}_t^{(j)}$  with an objective:

$$\mathcal{L}(\mathbf{v}_i, \mathbf{t}_i^+, \mathbf{t}_i^-) = \mathcal{L}_{ce}(\mathbf{v}_i, \mathbf{t}_i^+) + \lambda \mathcal{L}_{\text{triplet}}(\mathbf{v}_i, \mathbf{t}_i^+, \mathbf{t}_i^-) \quad (6)$$

where  $\mathbf{v}_i, \mathbf{t}_i^+$  and  $\mathbf{t}_i^-$  are the visual embedding, true class name, and negative class name embeddings corresponding to the segment  $i$ , and  $\mathcal{L}_t$  is a triplet loss [2].

$$\mathcal{L}_{\text{triplet}}(\mathbf{v}_i, \mathbf{t}_i^+, \mathbf{t}_i^-) = \max\{\|\mathbf{v}_i - \mathbf{t}_i^+\|_2 - \|\mathbf{v}_i - \mathbf{t}_i^-\|_2 + \mu, 0\} \quad (7)$$

and the margin  $\mu$  is set to 1.5. The triplet loss is applied to retain open-vocabulary segmentation capabilities while adapting to a specific domain, inspired by the contrastive objective from CLIP [39]. Note that, we gradually increase the  $\lambda$  in (6) from  $\lambda_{\min}$  to  $\lambda_{\max}$ .

## 4.4 Triplet Mining

**Negative Sample Database.** One of the challenges of employing triplet loss is to find proper negative samples to form triplets. Using triplets with randomly selected negative samples will get the optimization process stuck quickly, making it hard to converge. To address this issue, we instruct GPT-4 to generate 5 closely related queries for each query in the training dataset. These text phrases

should be difficult for a machine learning model to distinguish, but clearly distinct for humans. For instance, “wall” and “room divider” are hard to distinguish for models but have a semantic difference. We list detailed prompts for GPT-4 negative name generation in the supplement.

**Online Hard Negative Sample Mining.** After generating the negative database, we employ an online hard negative mining strategy to identify informative triplets with the hardest negatives during training, as outlined in [15, 40, 44, 56]. This approach is crucial for enhancing the model’s ability to differentiate between similar yet distinct classes, thereby increasing its precision. For a dataset with  $N$  classes, we find the hardest negative query for each segment on the fly from the remaining  $N - 1$  classes and generated negative queries. In particular, we find the hardest negative by the lowest  $L_2$  distance between its text embedding and the visual embedding  $\mathbf{v}_i$  of the target segment  $i$ . Combined with the segment’s class name and visual embedding, it forms the triplet to refine the text prompts.

#### 4.5 Application in Existing 2D & 3D Open-Vocabulary Segmentation Pipelines

After training OpenDAS with the described methodology, we apply it to existing open-vocabulary segmentation (OVS) pipelines, namely OVSeg [32] for images and OpenMask3D [45] for point clouds. Both follow the common architecture of Sec. 4.1 with a mask proposal generator followed by an open-vocabulary segment classification module. Our method can be integrated as a plug-and-play component into this module, replacing the previous image and text encoders.

### 5 Experiments

As defined in Section 3, the task of domain adaptation for OVS requires different data for adaptation training and for testing. The evaluation on the test data is further split into *base queries* that are also present during the adaptation training, and *novel queries* that test the zero-shot open-vocabulary understanding of the adapted model. As established in OVS literature, we conduct experiments on 2D and 3D segmentation datasets, using the annotated labels as queries.









**Datasets.** We use three datasets, covering indoor and outdoor domains: (i) ADE20K-150 [60, 61], (ii) KITTI-360 [33], and (iii) ScanNet++ Offices [57]. ADE20K covers indoor and outdoor scenes with 2000 images for validation and 150 distinct classes. It is widely used to evaluate OVS models [5, 55, 58, 32, 37, 53]. KITTI-360 covers urban driving scenes in Germany with 37 semantic labels. ScanNet++ is a dataset with 450+ 3D indoor scenes including iPhone RGB-D streams.

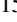
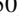
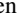

We construct a subset of ScanNet++ to specifically test generalization to novel queries, which we refer to as ScanNet++ Offices. For this, we visually identify 30 office scenes, covering different university rooms at TUM. We split this subset to test our model’s open-vocabulary classification capabilities. With 14 scenes for adaptation training (7989 images) and 16 scenes for testing (11054 images), we get a split of 156 training and 233 test labels, 108 of which are common. This allows us to test with 108 base and 125 novel queries. Please refer to the supplements for the scene IDs used for training and evaluation.









**Baselines.** In addition to our proposed method, we evaluate state-of-the-art prompt learning methods CoCoOp [64], VPT [19], RPO [27], and MaPLe [23]. These methods are usually evaluated on image classification, while we present results on OVS. Further comparisons against the WiSE-FT robust fine-tuning method [48] can be found in the supplementary material.

**Metrics.** To measure the adaptation performance with ground-truth masks, we use Accuracy (Acc), and a family of F1 scores, including Weighted-F1 (W-F1) by weighing the number of occurrences for each label, Base-F1 (B-F1) over base queries that are seen during adaptation training, and Novel-F1 (N-F1) over novel, unseen queries. In experiments with predicted masks, we measure the commonly used metrics mean IoU (mIoU) and the mean Accuracy (mAcc) for 2D OVS and AP (Average Precision),  $AP_{50}$  and  $AP_{25}$  for 3D OVS tasks.

**Implementation Details.** Following previous prompt learning approaches [65, 64, 23, 27], we use DSSL library [66, 63] to implement prompt tuning on CLIP with the triplet loss. We first optimize only the visual prompts for 5 epochs. During training, we have a warmup epoch with a learning rate of  $10^{-5}$  and then set the base learning rate to 0.0025 with a cosine scheduler from the second epoch. After training visual prompts, we only optimize the text prompts for another 5 epochs with the same base learning rate. We use a batch size of 16 and an SGD optimizer on a single NVIDIA A100 GPU, and the training time is around 10-15 hours in total depending on the dataset. The 2D segments excerpted from different datasets have filled background with the average pixel value of CLIP training images as done in [32]. The  $\lambda_{\min}$  and  $\lambda_{\max}$  is set to be 2 and 5, respectively.

Method	Modality	# Params	SN++ Office		KITTI-360		ADE20K-150	
			Acc	W-F1	Acc	W-F1	Acc	W-F1
No adaptation		0	9.0	11.2	19.1	23.4	27.8	32.7
CoCoOp [64]		~ 77K	28.9	25.7	61.1	59.7	54.2	51.8
VPT [19]		~ 786K	29.3	33.8	65.2	67.7	58.2	59.8
RPO [27]	 	~ 43K	35.4	30.6	66.0	63.6	58.1	55.2
MaPLe [23]	 	~ 18935K	38.9	36.3	69.9	68.6	67.7	65.9
OpenDAS (Ours)	 	~ 233K	<b>43.7</b>	<b>40.2</b>	<b>75.7</b>	<b>75.2</b>	<b>73.1</b>	<b>71.9</b>

**Table 1: Parameter-Efficient Domain Adaptation for Segment Classification.** We evaluate segment classification with adapted VLMs on indoor data (ScanNet++ Office), outdoor data (KITTI-360), and a combination of both domains (ADE20K-150). Baseline methods adapt the text encoder, , the visual encoder, , or both modalities,  . # Params denote the number of learnable parameters. Our approach shows the best adaptation ability on all datasets.

Method	Modality	# Params	SN++ Office			A-150 → SN++ O			A-150 → K-360		
			W-F1	B-F1	N-F1	W-F1	B-F1	N-F1	W-F1	B-F1	N-F1
No adaptation		0	11.2	11.0	12.0	11.2	11.3	11.0	24.1	23.0	24.9
CoCoOp [64]		~ 77K	25.7	34.3	12.7	11.2	18.0	9.9-1.1	27.1	30.4	22.1-2.8
VPT [19]		~ 786K	33.8	37.6	12.8	13.0	19.2	8.8-2.2	29.5	34.8	25.8
RPO [27]	 	~ 43K	30.6	40.9	14.9	13.4	13.9	13.3	33.7	42.8	19.9-5.0
MaPLe [23]	 	~ 18935K	36.3	48.1	18.4	18.8	29.3	16.8	43.5	57.7	22.2-2.7
OpenDAS (Ours)	 	~ 233K	<b>40.2</b>	<b>51.5</b>	<b>23.0</b>	<b>23.0</b>	<b>30.4</b>	<b>21.6</b>	<b>47.1</b>	<b>60.8</b>	<b>26.6</b>

**Table 2: Open-Vocabulary Understanding.** We evaluate segment classification over base queries that have also been part of the adaptation training (B-F1) as well as generalization to unseen, novel queries (N-F1) and the overall weighed F1 (W-F1). To be able to test on novel queries, we evaluate on ScanNet++ Offices (SN++ O) and cross-dataset by adapting to ADE20K-150 (A-150) and testing on SN++ O and KITTI-360 (K-360). Performance degradation compared to the original CLIP baseline is shown in red.

## 5.1 Main Results

**Parameter-Efficient Domain Adaptation for Segment Classification.** We commence our analysis by integrating CLIP into the 2D segment classification task, thereby augmenting the efficacy of the overall open-vocabulary segmentation process. The results of prompt learning on segment classification are detailed in Table 1. Prompt learning techniques in general improve CLIP’s segment classification capabilities in the target domain significantly. However, the baseline multimodal approaches like RPO and MaPLe trained with the cross-entropy loss do not necessarily outperform VPT, which only adapts in the visual domain. This is due to the inherently greedy nature of cross-entropy loss, impacting CLIP’s intra-class representation and open-vocabulary generalization.

**Open-Vocabulary Understanding.** To further evaluate the capability for open-vocabulary segment classifications, we set up 125 unseen novel classes for ScanNet++ Offices. As illustrated in Table 2, the original CLIP is indifferent to base and novel classes. Baseline methods exhibit noticeable performance boosts over the original CLIP on the W-F1 and B-F1, but only marginally improve upon the N-F1 metric. In contrast, we demonstrate superior performance on all three metrics. Similarly, when trained on ADE20K-150 and evaluated cross-dataset, significant improvements over all baselines were observed, especially for novel classes. Across the three evaluations in Table 2, OpenDAS consistently achieves a higher N-F1 than the original CLIP. In contrast, other methods occasionally show a decrease in open-vocabulary generalization following adaptation. This suggests that the triplet loss effectively preserves the structured embedding space while the adaptation process closes the domain gap between CLIP’s training images and the target data.

**Benefit of Domain Adaptation in Open-Vocabulary Segmentation.** Besides evaluating our segment classification performance given GT masks, we apply our prompt tuning method to OVSeg [32] and OpenMask3D [45]’s predicted masks, assessing whether our method can help them better understand the semantics of each segment. As shown in Table 3, we observe the performance boost in all metrics when applying our method to OVSeg and OpenMask3D. Our method shows especially significant improvements with lower IoU thresholds than the original OpenMask3D. This demonstrates that OpenDAS can be directly incorporated into different OVS pipelines.

**Qualitative Comparisons.** We present the qualitative results on ScanNet++ Offices [57], KITTI-360 [33], and ADE20K [60, 61] in Fig. 4. Our method shows clear improvements over CLIP,

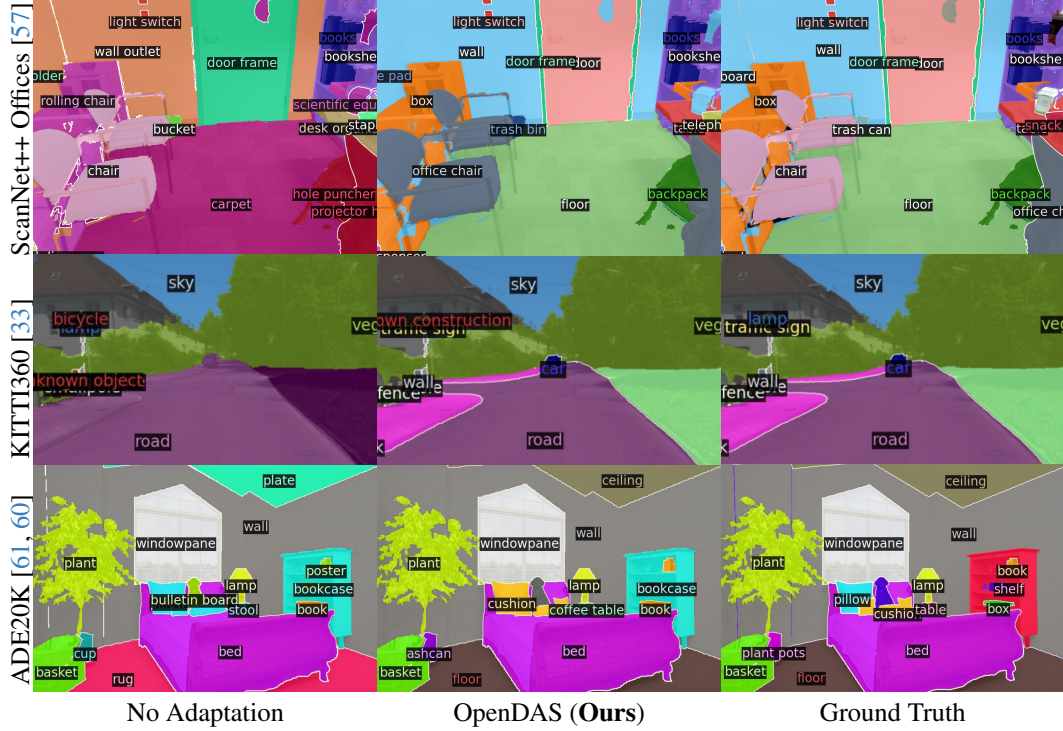


**Figure 4: Qualitative Comparison on Segment Classification.** We show the predicted object classes with the ground truth masks given on three datasets.

Method	ADE20K-150		Method	ScanNet++ Offices		
	mIoU (%)	mAcc (%)		AP	AP <sub>50</sub>	AP <sub>25</sub>
OVSeg [32]	29.8	48.1	OpenMask3D [45]	8.1	11.5	14.1
+ OpenDAS	<b>35.8</b> +6.0	<b>51.2</b> +3.1	+ OpenDAS	<b>12.2</b> +4.1	<b>18.0</b> +6.5	<b>24.0</b> +9.9

**Table 3: Benefit of Domain Adaptation in Open-Vocabulary Segmentation.** We apply our method to recent open-vocabulary 2D semantic segmentation model OVSeg [32] and SOTA open-vocabulary 3D instance segmentation model OpenMask3D [45]. Our method boosts their performance with only their predicted masks.

$\lambda_{\max}$	SN++ Offices		KITTI-360		ADE20K-150		Training Setting		SN++ Offices	KITTI360	ADE20K
	Acc	W-F1	Acc	W-F1	Acc	W-F1	Stage 1	Stage 2			
0	38.9	34.8	66.4	64.4	51.7	48.4	Joint + T		39.9	36.2	72.3
2	39.8	35.8	71.9	70.2	55.8	54.0	👉 + T		33.9	29.9	72.5
5	<b>40.1</b>	<b>36.5</b>	<b>72.9</b>	<b>70.9</b>	<b>65.7</b>	<b>63.6</b>	👉 + T		42.3	38.8	71.9
10	39.3	35.7	72.1	70.8	58.9	56.5	👉 + T		<b>43.7</b>	<b>40.2</b>	<b>75.7</b>

**Table 4: Ablation on Maximum Triplet Loss Weight ( $\lambda_{\max}$ ) and Training Setting.** OpenDAS comparison with different  $\lambda_{\max}$  and prompt depth  $J=12$  (left) and training settings (right). Triplet loss is denoted as +T.

distinguishing classes like “door frame” - “door”, “road” - “sidewalk”, “plate” - “ceiling”. Fig. 5 demonstrates how OpenDAS can boost the performance of OpenMask3D [45] by switching out the VLM. The improvement in seen classes like “wall socket” is anticipated. However, as OpenDAS is adapted to predict from the masked images, it improves predictions on novel queries like “robot arm”.

## 5.2 Ablation Studies

$\lambda_{\max}$ . Setting  $\lambda_{\max} = 0$  indicates that the training objective in Eq. (6) for text prompts defaults to only cross-entropy loss as the objective. As  $\lambda_{\max}$  increases, the weight for triplet loss also increases during training. The left side of Table 4 shows that the performance has a peak when we set  $\lambda_{\max} = 5$  for both datasets, so we choose it as our default value.

**Training Setting.** RPO [27] suggests that the image and text encoders should be trained together. Our ablation however shows that with the triplet loss, a 2-stage training of first visual prompt optimization (👉), followed by textual prompt optimization (👉 + T) achieves the highest performance.



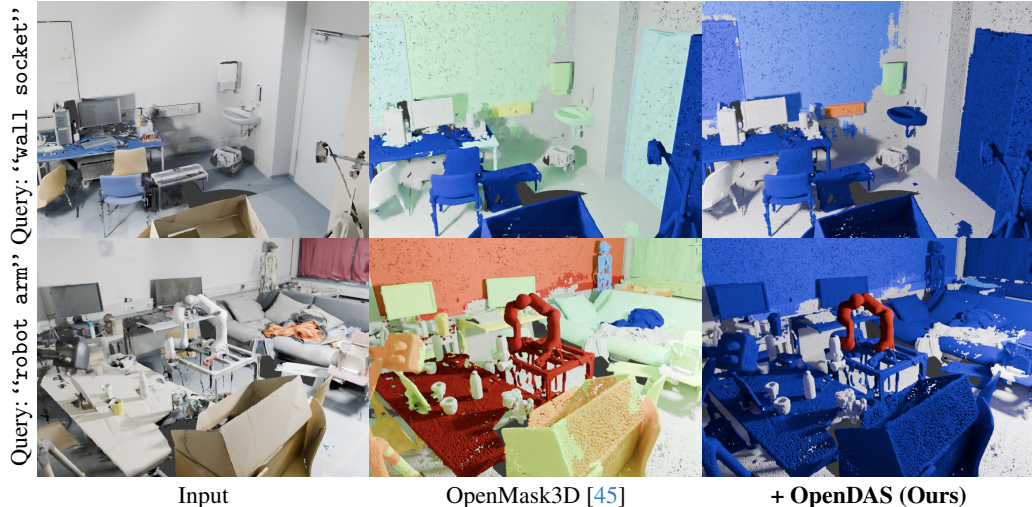


**Figure 5: Qualitative Comparison on Open-Vocabulary 3D Instance Segmentation.** We show the query-response scores of OpenMask3D [45] masks predicted with CLIP [39] and OpenDAS. Blue indicates low similarity with the text query and red high similarity. Unlike the original CLIP, OpenDAS can match the correct mask with the query with a strong similarity score.

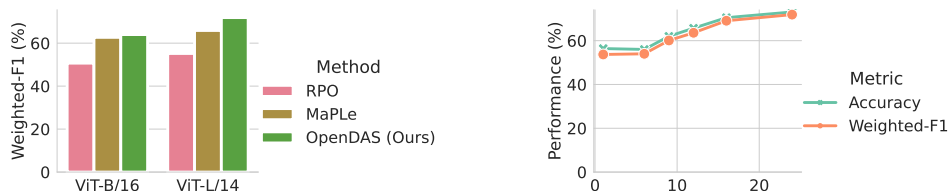


**Figure 6: Ablations on ViT Backbone and Prompt Depth ( $J$ ) on ADE20K-150 [60, 61].** On the left figure, ViT-L/14 (307M parameters) is significantly larger than ViT-B/16 (86M parameters). This larger backbone boosts the performance of all methods over ADE20K. The right figure reveals that adding prompts to more layers improves the performance of OpenDAS.

**ViT Backbone.** We present a comparison on the visual backbone and its impact on the accuracy on the left side of Fig. 6. We observe that with all methods, performance increases with a larger backbone. Thus, we use ViT-L/14 for all our experiments, unlike prior prompt learning methods. We refer the readers to the supplementary material for the ablations on other datasets.

**Prompt Depth.** When  $J = 1$ , we only add prompts in the input space, and the larger  $J$  is, the more layers we add learnable prompts to. When  $J = 24$ , we add prompts to all layers. We observe that OpenDAS improves with an increase of  $J$ . Hence, we adopt  $J = 24$  as the standard setting. We refer the readers to the supplementary material for the ablations on other datasets.

## 6 Conclusion & Limitations

We show that prompt tuning methods, especially when combined with triplet loss, can significantly enhance VLMs’ performance for open-vocabulary segmentation tasks in a parameter-efficient way. Our custom training scheme with triplet loss improves adaptation, achieving better results in both base and novel classes. Applying our model with ground-truth masks to different datasets yields significant improvements over previous methods, demonstrating the efficacy of triplet loss. Integrating our method into existing OVS pipelines boosts performance in both 2D and 3D OVS tasks.

Despite promising results, our work has limitations. All evaluated methods require annotated ground-truth segmentation, which is expensive to obtain. Future work could explore few-shot learning settings for domain adaptation for OVS, increasing practicality for the real-world applications. While parameter-efficient, prompt tuning still lags behind robust fine-tuning in generalizing to novel queries. Finally, our experiments were limited as most datasets for domain adaptation share the same annotated classes, making it difficult to capture generalization to unseen queries in a defined visual domain.



## References

- [1] Josh Achiam, Steven Adler, Sandhini Agarwal, Lama Ahmad, Ilge Akkaya, Florencia Leoni Aleman, Diogo Almeida, Janko Altschmidt, Sam Altman, Shyamal Anadkat, et al. Gpt-4 technical report. *arXiv preprint arXiv:2303.08774*, 2023. 14
- [2] Vassileios Balntas, Edgar Riba, Daniel Ponsa, and Krystian Mikolajczyk. Learning local feature descriptors with triplets and shallow convolutional neural networks. In *BMVC*, 2016. 5
- [3] Haoran Chen, Kenneth Blomqvist, Francesco Milano, and Roland Siegwart. Panoptic vision-language feature fields. *IEEE Robotics and Automation Letters*, 2024. 3
- [4] Bowen Cheng, Alexander G. Schwing, and Alexander Kirillov. Per-Pixel Classification is Not All You Need for Semantic Segmentation. In *NeurIPS*, 2021. 17
- [5] Seokju Cho, Heeseong Shin, Sunghwan Hong, Seungjun An, Seungjun Lee, Anurag Arnab, Paul Hongsuck Seo, and Seungryong Kim. Cat-seg: Cost aggregation for open-vocabulary semantic segmentation, 2023. 3, 6
- [6] Alexandros Delitzas, Ayca Takmaz, Federico Tombari, Robert Sumner, Marc Pollefeys, and Francis Engelmann. SceneFun3D: Fine-Grained Functionality and Affordance Understanding in 3D Scenes. In *CVPR*, 2024. 1
- [7] Jian Ding, Nan Xue, Gui-Song Xia, and Dengxin Dai. Decoupling zero-shot semantic segmentation. In *CVPR*, 2022. 3
- [8] Zheng Ding, Jieke Wang, and Zhuowen Tu. Open-vocabulary universal image segmentation with maskclip. In *ICML*, 2023. 3
- [9] Francis Engelmann, Fabian Manhardt, Michael Niemeyer, Keisuke Tateno, and Federico Tombari. OpenNeRF: Open Set 3D Neural Scene Segmentation with Pixel-Wise Features and Rendered Novel Views. In *ICLR*, 2024. 3
- [10] Abolfazl Farahani, Sahar Voghoei, Khaled Rasheed, and Hamid Arabnia. A brief review of domain adaptation, 2020. 3
- [11] Yulu Gan, Yan Bai, Yihang Lou, Xianzheng Ma, Renrui Zhang, Nian Shi, and Lin Luo. Decorate the newcomers: Visual domain prompt for continual test time adaptation. *AAAI*, 37, 2023. 2, 3
- [12] Yunhe Gao, Xingjian Shi, Yi Zhu, Hao Wang, Zhiqiang Tang, Xiong Zhou, Mu Li, and Dimitris N. Metaxas. Visual prompt tuning for test-time domain adaptation, 2023. 2, 3
- [13] Golnaz Ghiasi, Xiuye Gu, Yin Cui, and Tsung-Yi Lin. Scaling open-vocabulary image segmentation with image-level labels. In *ECCV*, 2022. 2
- [14] Yuxian Gu, Xu Han, Zhiyuan Liu, and Minlie Huang. PPT: Pre-trained prompt tuning for few-shot learning. In Smaranda Muresan, Preslav Nakov, and Aline Villavicencio, editors, *Proceedings of the 60th Annual Meeting of the Association for Computational Linguistics (Volume 1: Long Papers)*, 2022. 3
- [15] Alexander Hermans, Lucas Beyer, and Bastian Leibe. In defense of the triplet loss for person re-identification. *arXiv preprint arXiv:1703.07737*, 2017. 6
- [16] Hao Huang, Jack Chu, and Fangyun Wei. Unsupervised prompt learning for vision-language models. *ArXiv*, abs/2204.03649, 2022. 3
- [17] Rui Huang, Songyou Peng, Ayca Takmaz, Federico Tombari, Marc Pollefeys, Shiji Song, Gao Huang, and Francis Engelmann. Segment3d: Learning fine-grained class-agnostic 3d segmentation without manual labels. *arXiv*, 2024. 3
- [18] Chao Jia, Yinfei Yang, Ye Xia, Yi-Ting Chen, Zarana Parekh, Hieu Pham, Quoc Le, Yun-Hsuan Sung, Zhen Li, and Tom Duerig. Scaling up visual and vision-language representation learning with noisy text supervision. In *ICML*, 2021. 1

- [19] Menglin Jia, Luming Tang, Bor-Chun Chen, Claire Cardie, Serge Belongie, Bharath Hariharan, and Ser-Nam Lim. Visual prompt tuning. In *ECCV*, 2022. 2, 3, 5, 6, 7, 14, 15, 16, 17
- [20] Xin Jin, Cuiling Lan, Wenjun Zeng, and Zhibo Chen. Domain prompt tuning via meta relabeling for unsupervised adversarial adaptation. *IEEE Transactions on Multimedia*, 2023. 2, 3
- [21] Justin Kerr, Chung Min Kim, Ken Goldberg, Angjoo Kanazawa, and Matthew Tancik. LERF: Language Embedded Radiance Fields. In *ICCV*, 2023. 3
- [22] Muhammad Uzair khattak, Muhammad Ferjad, Naseer Muzzamal, Luc Van Gool, and Federico Tombari. Learning to prompt with text only supervision for vision-language models. *arXiv:2401.02418*, 2024. 2, 3
- [23] Muhammad Uzair Khattak, Hanoona Rasheed, Muhammad Maaz, Salman Khan, and Fahad Shahbaz Khan. Maple: Multi-modal prompt learning. In *CVPR*, 2023. 3, 5, 6, 7, 14, 15, 16, 17
- [24] Muhammad Uzair Khattak, Syed Talal Wasim, Muzammal Naseer, Salman Khan, Ming-Hsuan Yang, and Fahad Shahbaz Khan. Self-regulating prompts: Foundational model adaptation without forgetting. In *ICCV*, 2023. 2, 3
- [25] Sosuke Kobayashi, Eiichi Matsumoto, and Vincent Sitzmann. Decomposing nerf for editing via feature field distillation. In *NeurIPS*, 2022. 3
- [26] Lars Kreuzberg, Idil Esen Zulfikar, Sabarinath Mahadevan, Francis Engelmann, and Bastian Leibe. 4d-stop: Panoptic segmentation of 4d lidar using spatio-temporal object proposal generation and aggregation. In *European Conference on Computer Vision Workshops (ECCVW)*, 2022. 3
- [27] D. Lee, S. Song, J. Suh, J. Choi, S. Lee, and H. J. Kim. Read-only prompt optimization for vision-language few-shot learning. In *ICCV*, 2023. 2, 3, 5, 6, 7, 8, 14, 15, 16, 17
- [28] Oliver Lemke, Zuria Bauer, René Zurbrügg, Marc Pollefeys, Francis Engelmann, and Hermann Blum. Spot-compose: A framework for open-vocabulary object retrieval and drawer manipulation in point clouds. In *2nd Workshop on Mobile Manipulation and Embodied Intelligence at ICRA*, 2024. 1
- [29] Brian Lester, Rami Al-Rfou, and Noah Constant. The power of scale for parameter-efficient prompt tuning. In Marie-Francine Moens, Xuanjing Huang, Lucia Specia, and Scott Wen-tau Yih, editors, *Proceedings of the 2021 Conference on Empirical Methods in Natural Language Processing*, 2021. 3
- [30] Boyi Li, Kilian Q Weinberger, Serge Belongie, Vladlen Koltun, and Rene Ranftl. Language-driven semantic segmentation. In *ICLR*, 2022. 2
- [31] Xiang Lisa Li and Percy Liang. Prefix-tuning: Optimizing continuous prompts for generation. In *Proceedings of the 59th Annual Meeting of the Association for Computational Linguistics and the 11th International Joint Conference on Natural Language Processing (Volume 1: Long Papers)*, 2021. 3
- [32] Feng Liang, Bichen Wu, Xiaoliang Dai, Kunpeng Li, Yanan Zhao, Hang Zhang, Peizhao Zhang, Peter Vajda, and Diana Marculescu. Open-vocabulary semantic segmentation with mask-adapted clip. In *CVPR*, 2023. 3, 5, 6, 7, 8, 16, 17
- [33] Yiyi Liao, Jun Xie, and Andreas Geiger. KITTI-360: A novel dataset and benchmarks for urban scene understanding in 2d and 3d. *IEEE TPAMI*, 2022. 6, 7, 8, 14, 16
- [34] Peiqi Liu, Yaswanth Orru, Chris Paxton, Nur Muhammad Mahi Shafiullah, and Lerrel Pinto. Ok-robot: What really matters in integrating open-knowledge models for robotics. *arXiv preprint arXiv:2401.12202*, 2024. 1
- [35] Xiao Liu, Yanan Zheng, Zhengxiao Du, Ming Ding, Yujie Qian, Zhilin Yang, and Jie Tang. Gpt understands, too. *AI Open*, 2023. 3




- [36] Yang Miao, Francis Engelmann, Olga Vysotska, Federico Tombari, Marc Pollefeys, and Dániel Béla Baráth. SceneGraphLoc: Cross-Modal Coarse Visual Localization on 3D Scene Graphs. In *arXiv preprint arXiv:2404.00469*, 2024. 1
- [37] Muhammad Ferjad Naeem, Yongqin Xian, Xiaohua Zhai, Lukas Hoyer, Luc Van Gool, and Federico Tombari. Silc: Improving vision language pretraining with self-distillation. *arXiv preprint arXiv:2310.13355*, 2023. 6
- [38] Songyou Peng, Kyle Genova, Chiyu Jiang, Andrea Tagliasacchi, Marc Pollefeys, Thomas Funkhouser, et al. Openscene: 3d scene understanding with open vocabularies. In *CVPR*, 2023. 3
- [39] Alec Radford, Jong Wook Kim, Chris Hallacy, Aditya Ramesh, Gabriel Goh, Sandhini Agarwal, Girish Sastry, Amanda Askell, Pamela Mishkin, Jack Clark, et al. Learning transferable visual models from natural language supervision. In *ICML*, 2021. 1, 3, 4, 5, 9
- [40] Florian Schroff, Dmitry Kalenichenko, and James Philbin. FaceNet: A Unified Embedding for Face Recognition and Clustering. In *CVPR*, 2015. 6
- [41] Jonas Schult, Francis Engelmann, Alexander Hermans, Or Litany, Siyu Tang, and Bastian Leibe. Mask3d: Mask transformer for 3d semantic instance segmentation. In *ICRA*, 2023. 3
- [42] Dhruv Shah, Michael Robert Equi, Błażej Osiniński, Fei Xia, Brian Ichter, and Sergey Levine. Navigation with large language models: Semantic guesswork as a heuristic for planning. In *Conference on Robot Learning*, 2023. 1
- [43] Sheng Shen, Shijia Yang, Tianjun Zhang, Bohan Zhai, Joseph E Gonzalez, Kurt Keutzer, and Trevor Darrell. Multitask vision-language prompt tuning. In *WACV*, 2024. 3
- [44] Edgar Simo-Serra, Eduard Trulls, Luis Ferraz, Iasonas Kokkinos, Pascal Fua, and Francesc Moreno-Noguer. Discriminative learning of deep convolutional feature point descriptors. In *ICCV*, 2015. 6
- [45] Ayça Takmaz, Elisabetta Fedele, Robert W. Sumner, Marc Pollefeys, Federico Tombari, and Francis Engelmann. OpenMask3D: Open-Vocabulary 3D Instance Segmentation. In *NeurIPS*, 2023. 3, 6, 7, 8, 9
- [46] Ayça Takmaz, Jonas Schult, Irem Kaftan, Mertcan Akçay, Bastian Leibe, Robert Sumner, Francis Engelmann, and Siyu Tang. 3D Segmentation of Humans in Point Clouds with Synthetic Data. In *ICCV*, 2023. 3
- [47] Silvan Weder, Hermann Blum, Francis Engelmann, and Marc Pollefeys. LabelMaker: Automatic Semantic Label Generation from RGB-D Trajectories. In *International Conference on 3D Vision (3DV)*, 2024. 3
- [48] Mitchell Wortsman, Gabriel Ilharco, Jong Wook Kim, Mike Li, Simon Kornblith, Rebecca Roelofs, Raphael Gontijo Lopes, Hannaneh Hajishirzi, Ali Farhadi, Hongseok Namkoong, and Ludwig Schmidt. Robust fine-tuning of zero-shot models. In *CVPR*, 2022. 6, 14
- [49] Jianzong Wu, Xiangtai Li, Shilin Xu, Haobo Yuan, Henghui Ding, Yibo Yang, Xia Li, Jiangning Zhang, Yunhai Tong, Xudong Jiang, Bernard Ghanem, and Dacheng Tao. Towards open vocabulary learning: A survey. *IEEE TPAMI*, 2024. 2, 3, 4
- [50] Jimmy Wu, Rika Antonova, Adam Kan, Marion Lepert, Andy Zeng, Shuran Song, Jeannette Bohg, Szymon Rusinkiewicz, and Thomas Funkhouser. Tidybot: Personalized robot assistance with large language models. *Autonomous Robots*, 2023. 1
- [51] Yuxin Wu, Alexander Kirillov, Francisco Massa, Wan-Yen Lo, and Ross Girshick. Detectron2. <https://github.com/facebookresearch/detectron2>, 2019. 17
- [52] Yan Xia, Letian Shi, Zifeng Ding, João F Henriques, and Daniel Cremers. Text2loc: 3d point cloud localization from natural language. *arXiv preprint arXiv:2311.15977*, 2023. 1

- [53] Bin Xie, Jiale Cao, Jin Xie, Fahad Shahbaz Khan, and Yanwei Pang. Sed: A simple encoder-decoder for open-vocabulary semantic segmentation. *arXiv preprint arXiv:2311.15537*, 2023. 6
- [54] Jiarui Xu, Sifei Liu, Arash Vahdat, Wonmin Byeon, Xiaolong Wang, and Shalini De Mello. Open-Vocabulary Panoptic Segmentation with Text-to-Image Diffusion Models. *arXiv preprint arXiv:2303.04803*, 2023. 3
- [55] Mengde Xu, Zheng Zhang, Fangyun Wei, Han Hu, and Xiang Bai. Side adapter network for open-vocabulary semantic segmentation. In *CVPR*, pages 2945–2954, 2023. 6
- [56] Hong Xuan, Abby Stylianou, and Robert Pless. Improved embeddings with easy positive triplet mining. In *WACV*, 2020. 6
- [57] Chandan Yeshwanth, Yueh-Cheng Liu, Matthias Nießner, and Angela Dai. Scannet++: A high-fidelity dataset of 3d indoor scenes. In *ICCV*, 2023. 6, 7, 8, 13, 15
- [58] Qihang Yu, Ju He, Xueqing Deng, Xiaohui Shen, and Liang-Chieh Chen. Convolutions die hard: Open-vocabulary segmentation with single frozen convolutional clip. *NeurIPS*, 36, 2024. 6
- [59] Yuanwen Yue, Sabarinath Mahadevan, Jonas Schult, Francis Engelmann, Bastian Leibe, Konrad Schindler, and Theodora Kontogianni. AGILE3D: Attention Guided Interactive Multi-object 3D Segmentation. In *ICLR*, 2024. 3
- [60] Bolei Zhou, Hang Zhao, Xavier Puig, Sanja Fidler, Adela Barriuso, and Antonio Torralba. Scene parsing through ade20k dataset. In *CVPR*, 2017. 6, 7, 8, 9, 14, 17
- [61] Bolei Zhou, Hang Zhao, Xavier Puig, Tete Xiao, Sanja Fidler, Adela Barriuso, and Antonio Torralba. Semantic understanding of scenes through the ade20k dataset. *IJCV*, 2019. 6, 7, 8, 9, 14, 17
- [62] Chong Zhou, Chen Change Loy, and Bo Dai. Extract free dense labels from clip. In *ECCV*, 2022. 3
- [63] Kaiyang Zhou, Ziwei Liu, Yu Qiao, Tao Xiang, and Chen Change Loy. Domain generalization: A survey. *IEEE TPAMI*, 2022. 6, 16
- [64] Kaiyang Zhou, Jingkang Yang, Chen Change Loy, and Ziwei Liu. Conditional prompt learning for vision-language models. In *CVPR*, 2022. 2, 3, 5, 6, 7, 16
- [65] Kaiyang Zhou, Jingkang Yang, Chen Change Loy, and Ziwei Liu. Learning to prompt for vision-language models. *IJCV*, 2022. 2, 3, 5, 6, 16
- [66] Kaiyang Zhou, Yongxin Yang, Yu Qiao, and Tao Xiang. Domain adaptive ensemble learning. *IEEE Transactions on Image Processing*, 2021. 6, 16
- [67] René Zurbrugg, Yifan Liu, Francis Engelmann, Suryansh Kumar, Marco Hutter, Vaishakh Patil, and Fisher Yu. Icgnet: A unified approach for instance-centric grasping. In *ICRA*, 2024. 1

## A Further Qualitative Results against Prior Prompt Tuning Methods

In the provided figures (see Fig. 7, Fig. 8, Fig. 9), we compare our method’s segment classification capabilities over the other baseline methods, as well as the ground truth labels for reference.

Fig. 7 presents a qualitative comparison on ScanNet++ [57]. Our method, OpenDAS, displays robustness in classifying basic elements like “wall”, “floor”, and “whiteboard” across various view-points. OpenDAS adeptly differentiates between conceptually similar objects, for instance, “ceiling” - “ceiling beam” and “wall” - “objects” – a distinction that poses a challenge for other methods and is likely encouraged by our triplet loss. However, some failures remain, e.g., “object” instead of “kettle” in the first column, and instead of “window frame” in the second column.

Method	Modality	# Params	time/iter	SN++ Office			KITTI-360		ADE20K-150	
				W-F1	B-F1	N-F1	Acc	W-F1	Acc	W-F1
No adaptation		0		11.2	11.0	12.0	19.1	23.4	27.8	32.7
WiSE-FT [48]		~ 123M	0.85 s	31.0	35.0	29.5	53.9	58.8	47.9	51.0
WiSE-FT [48]		~ 304M	1.05 s	<b>45.9</b>	47.3	<b>45.3</b>	<b>78.8</b>	<b>80.5</b>	<b>73.9</b>	<b>74.8</b>
OpenDAS (Ours)		~ 233K	<b>0.53 s</b>	40.2	<b>51.5</b>	23.0	75.7	75.2	73.1	71.9

**Table 5: Comparison with Robust Fine-Tuning [48] on ScanNet++ Office, KITTI-360, and ADE20K-150.** We can see that we significantly outperform the text-encoder fine-tuning setting on all three datasets with about  $1000\times$  fewer parameters. We also present competitive results over their image-encoder fine-tuning setting that uses over  $2000\times$  more parameters, and show stronger B-F1 results on ScanNet++, while being  $2\times$  faster to train.

For KITTI-360 [33], we present comparisons in Fig. 8. The task is relatively simpler as we have only 37 semantic classes. Among these, several adapted models struggle to separate “road” from “sidewalk”, especially in instances where they share similar coloration. OpenDAS, leveraging the nuanced capabilities provided by triplet loss during training, successfully identifies and segregates these analogous classes.

In Fig. 9, we present a qualitative comparison on the ADE20K-150 dataset [61, 60]. As the task is closed-set with 150 classes, all prompt learning methods perform generally accurately on this dataset. However, we see that in some cases, multi-modal prompt tuning as done in RPO [27] and MaPLe [23] can result in a degradation in CLIP’s original representations, leading to occasional misclassification between “sky” and other entities, unlike VPT [19] and OpenDAS, which employ isolated visual prompt tuning. Similarly, we observe some other failures with distinguishing “table” and “chair” in the second column by other methods and “grass” from other classes. OpenDAS, while generally proficient, is not without its faults, as evidenced by the occasional inability to discriminate “grass” from “earth” or the misidentification of a glass door as a “mirror”.

## B Comparison Against Robust Fine-Tuning Method WiSE-FT [48]

We further compare our approach against a robust fine-tuning method that fine-tunes the entire CLIP text and visual encoder, respectively. It differs from standard fine-tuning as it ensembles the weights of pre-trained and fine-tuned model weights to keep the pre-trained model’s generalization capabilities. We show comparisons in Table 5 on KITTI-360 and ADE20K on the closed-vocabulary setting, as well as ScanNet++ Office dataset on the open-vocabulary setting. When compared to fine-tuning the CLIP text encoder, we achieve significant improvements in all metrics and all three datasets by only training  $\sim 0.1\%$  of CLIP-text encoder parameters. Looking into the comparison over fine-tuning the visual encoder, we show competitive results with only  $\sim 0.05\%$  of the parameters, and achieve significant improvements on base classes in the ScanNet++ Office dataset.

## C Negative Database for Triplet Loss

When triplet loss is trained with easy negatives, the learned latent space is likely to be suboptimal, not being able to distinguish similar classes and not generalizing well to unseen classes. By creating a negative database, we augment the set of negative classes to distinguish from.

For this purpose, we use GPT-4 [1] to generate 5 negatives for each class. We give the following instructions.

“Your task is to produce five distinct examples for each class provided in the list, ensuring that the examples are not subcategories of each other but rather represent clear and separate entities within the same class. This means that each example should not be a subset or type of another example within the same category. The objective is to create similar examples that might be confused by a machine learning model but remain discernible to a human observer to be used as clear negative examples for triplet loss training. The output format should be a Python dictionary for easy integration.”

Some examples of the generated classes are as follows.





**Figure 7: Qualitative Comparison on Segment Classification on ScanNet++ Offices [57].** We show the object classes with the ground truth masks predicted by baselines and OpenDAS, and ground truth labels. The masks are colored based on the class ID. On the contrary to existing methods, our model can give the closest match to the ground truth labels exhibiting a similar color pattern.

- ‘wall’: [‘room divider’, ‘partition’, ‘divider screen’, ‘privacy screen’, ‘decorative panel’]
- ‘ceiling’: [‘chandelier’, ‘pendant light’, ‘skylight’, ‘light fixture’, ‘ceiling fan’]
- ‘folder organizer’: [‘bedside table’, ‘end table’, ‘chest of drawers’, ‘bar stool’, ‘storage ottoman’]

During training, we choose the hardest negative for each sample among all the training and negative classes combined to optimize the triplet loss.

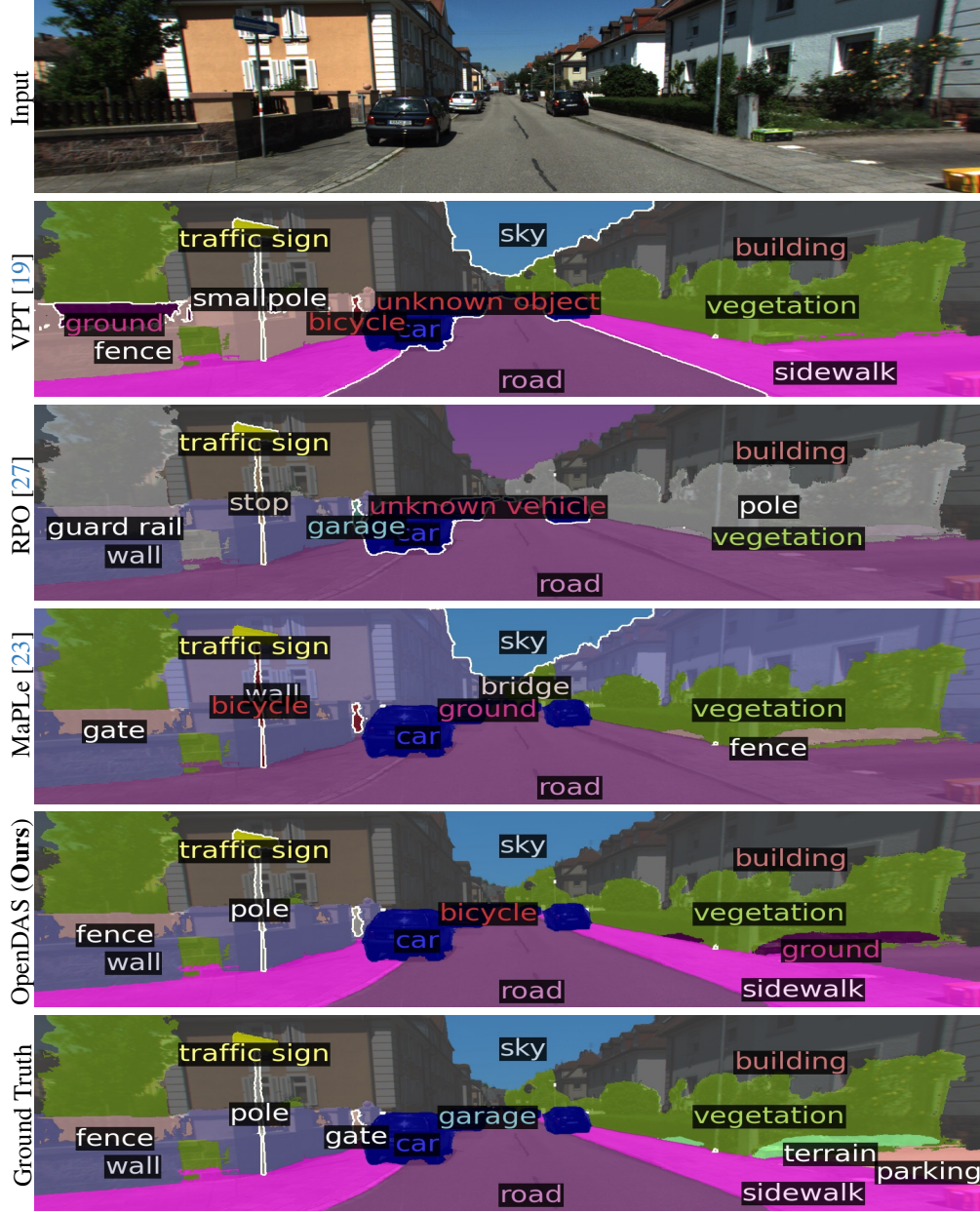


**Figure 8: Qualitative Comparison on Segment Classification on KITTI-360 Dataset [33].** We show the predicted object classes with the ground truth masks given on three datasets. The masks are colorized based on the class ID. Unlike the existing methods, our model can give the closest match to the ground truth labels understanding the distinction between ‘road’ and ‘sidewalk’.

## D Further Implementation Details

For the OpenDAS training pipeline, we first prepare segmentation datasets for the training of segment classification. Assuming that we have the 2D images as well as semantic annotations, we perform pre-processing on the dataset to adapt the semantic annotations to the classification task. As illustrated in Fig. 10, ground truth segmentation masks are applied, and the background is filled with the mean pixel values from CLIP’s original training images, mirroring the approach adopted by a prior open-vocabulary segmentation work, OVSeg [32]. Each segment is annotated with a unique ID to facilitate the classification task.

Having prepared the training set, we employ the Dassel library [66, 63] to train our prompt learning approach, adhering to the conventions established by prior prompt learning methodologies [65, 64,



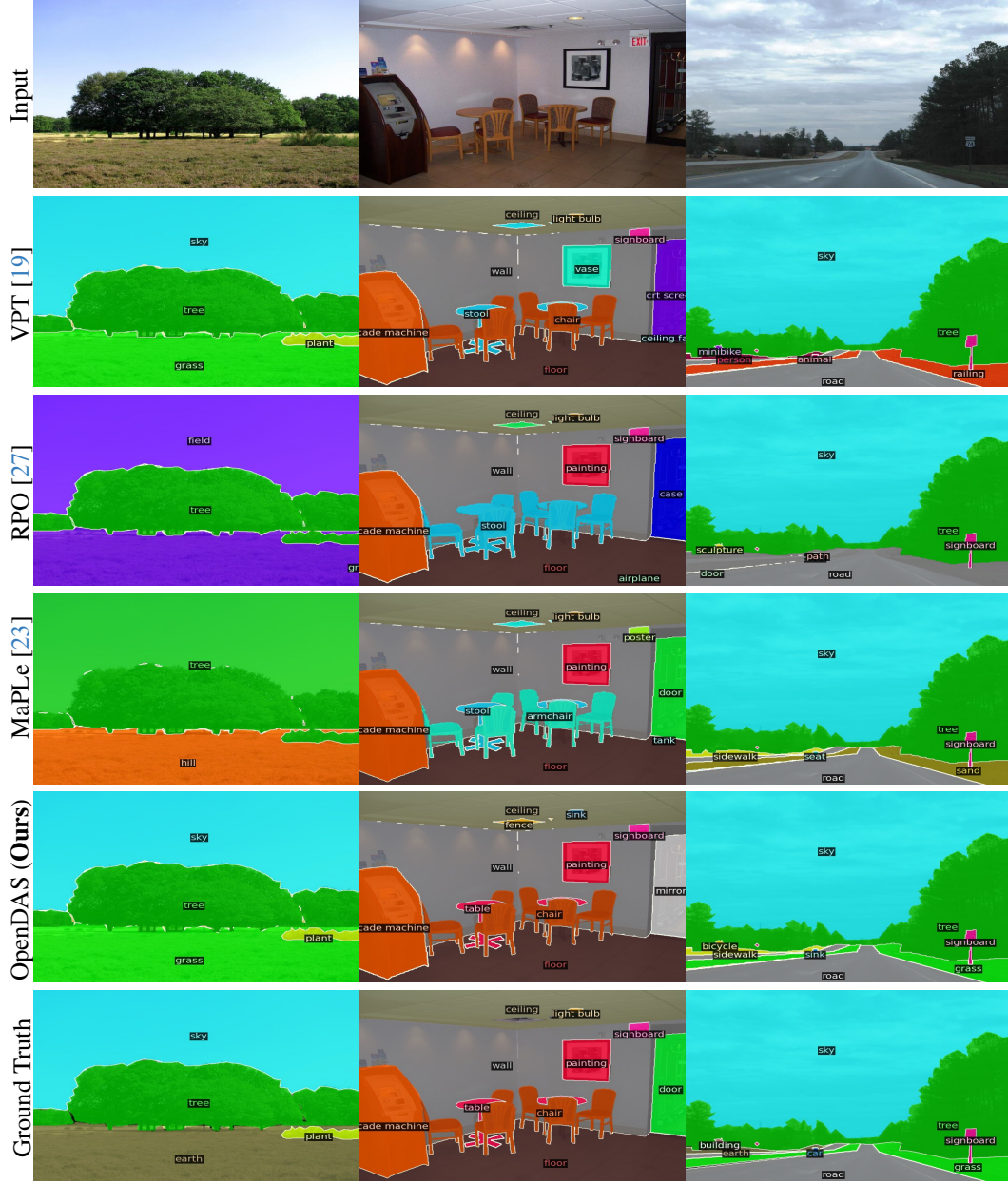


**Figure 9: Segment Classification Qualitative Comparison on ADE20K Dataset [61, 60].** We show the object classes with the ground truth masks predicted by baselines and OpenDAS, as well as ground truth labels. The masks are colored based on the class ID. We observe some improvements in the classification, exhibiting closer color patterns to the Ground Truth labels compared to other baselines.

[23, 27]. This way, we ensure compatibility with other baselines. We perform the inference with the same library and report the classification results measured with this implementation.

For class prediction with ground truth masks on a given image, we seamlessly integrate our tailored CLIP model with learned prompts into a segmentation framework built upon Detectron2 [51]. This segmentation pipeline is based on OVSeg [32], thereby enabling the integration of our customized CLIP model into the OVSeg pipeline. This integration allows us to use class-agnostic mask predictions that come from MaskFormer [4], as well as ground truth masks.



**Figure 10: Training Images.** We prepare classification annotations for the segment classification task by applying ground truth masks on images, where the background is filled with the mean pixel values from the original CLIP training images. Each segment is annotated with a unique ID for the classification task.

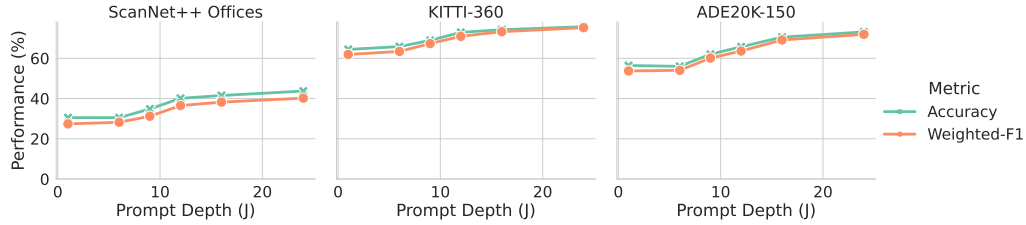


**Figure 11: Prompt Depth.** We compare different prompt depth values on the ScanNet++ Offices, KITTI-360, and ADE20K-150 validation splits. Our further analysis reveals that the more layers we add prompts, the better OpenDAS performs.

## E ScanNet++ Offices

In this section, we provide more details about the ScanNet++ Office scenes, with 14 scenes for training and 16 for testing.

- Training scenes: ["0b031f3119", "1204e08f17", "260fa55d50", "394a542a19", "39f36da05b", "40b56bf310", "4ba22fa7e4", "75d29d69b8", "8b5caf3398", "1366d5ae89", "1a8e0d78c0", "2a496183e1", "30f4a2b44d", "419cbe7c11"]
- Test scenes: ["4a1a3a7dc5", "56a0ec536c", "59e3f1ea37", "7cd2ac43b4", "8d563fc2cc", "8e00ac7f59", "98b4ec142f", "9b74afd2d2", "9f139a318d", "e91722b5a3", "94ee15e8ba", "07f5b601ee", "2e74812d00", "036bce3393", "260db9cf5a", "28a9ee4557"]

## F Further Ablation Studies

**Prompt Depth.** We compare different prompt depth values on the ScanNet++ Offices, KITTI-360, and ADE20K-150 validation splits in Fig. 11. Our further analysis reveals that the more layers we add prompts, the better OpenDAS performs over all datasets.

**ViT Backbone.** We present a comparison on the visual backbone and its impact on the accuracy in Fig. 12. We observe that with all multi-modal prompt learning methods, the performance increases with the larger backbone. Hence, we set ViT-L/14 for all our experiments contrary to the prior prompt learning methods standard settings.

**Number of Learnable Prompts (K).** This determines the number of prompts injected at each layer, or in other words, the ‘width’ of the prompts. In Table 6, we observe that we can gain additional improvement by adding more learnable prompts to the visual encoder for the ScanNet++ Office subset and ADE20K-150 validation set. We see that this parameter needs to be tuned for each dataset.

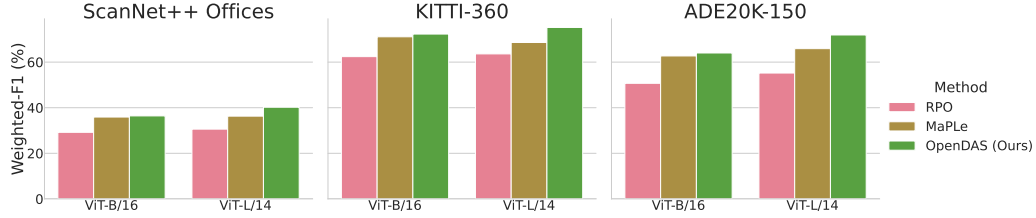


**Figure 12: ViT Backbone.** We compare different ViT backbones on ScanNet++ Offices, KITTI-360, and ADE20K-150 validation splits to observe their impact on performance. ViT-L/14 is significantly larger with 307M parameters compared to ViT-B/16 with 86M parameters. Results show that using a larger backbone boosts the performance in all methods over all datasets. Further analysis reveals that adding more layers of prompts improves the performance of OpenDAS.

K 🌈	K 🟦	# Params	ScanNet++		KITTI-360		ADE20K-150	
			Acc	W-F1	Acc	W-F1	Acc	W-F1
8	4	~ 135K	40.1	36.5	<b>72.9</b>	<b>70.9</b>	65.7	63.6
8	8	~ 172K	39.6	35.5	72.0	70.4	59.3	57.2
8	12	~ 209K	39.7	37.0	72.3	70.9	57.5	55.2
12	4	~ 184K	<b>40.3</b>	<b>37.4</b>	72.4	70.7	70.1	68.5
12	8	~ 221K	39.6	36.7	72.7	71.5	<b>70.9</b>	<b>69.4</b>
12	12	~ 258K	39.6	37.2	72.3	71.1	70.4	68.4

**Table 6: Number of Learnable Prompts (K).** We compare OpenDAS with different numbers of learnable prompts on the Scannet++ Office subset, KITTI-360, and ADE20K-150 (when prompt depth  $J = 12$ ). We denote the prompt length for the visual encoder as K 🌈 and for the textual encoder as K 🟦.

However, we choose  $(K \text{ 🌈}, K \text{ 🟦}) = (8, 4)$  as the standard setting for simplicity and to keep the number of parameters minimal.